MULTI-TEMPORAL INSAR ANALYSIS OF WENJIAGOU LANDSLIDE USING DISTRIBUTED SCATTERERS

Chao Wang [*(1)], Zhengjia Zhang [(1), (2)], Hong Zhang [(1)], Yixian Tang [(1)]

[(1)] *Key Laboratory of Digital Earth Science, Institute of Remote Sensing and Digital Earth, CAS, Beijing, China, 100094, Email: wangchao@radi.ac.cn*

[(2)] *University of Chinese Academy of Sciences, Beijing, China, 100049, Email:zhangzj01@radi.ac.cn*

ABSTRACT

This paper presents a multi-temporal InSAR method to monitor landslide movement at wenjiagou using Distributed Scatterers (DS). In this study, TDX and TSX bistatic SAR data are processed to obtain high precision DEM of the pose-landslide. DSs are efficiently identified using classified information and statistical characteristics. A series of Radarsat-2 HH polarization images collected in Wenjiagou from 2014.6 to 2014.9 are used to generate the deformation of the giant landslide. The experimental results show that there are obvious ground movement detected in the depositing area of the landslide during the observation.

1. INTRODUCTION

On 12th May 2008, a magnitude 8.0 earthquake happened in Sichuan province, China. It was reported that 60000 landslides and rock collapsed were trigged by the great earthquake over mountain area. Wenjiagou landslide is one of the biggest landslides triggered by the Wenchuan great earthquake. After the landslide event, mass debris are deposited in the gully of Wenjiagou, which have become potential threaten to the safety of local people. Although some man-made constructions have been fixed to control the mass debris, they also could move in rainy season. Therefore it is urgently needed to monitor the deformation information of the landslide. Conventional field investigation methods， such as GPS and levelling method, are time-consuming and difficulty to monitor the movement of the landslide.

Synthetic aperture radar interferometry (InSAR) is a powerful technology for measuring ground deformation by analysing the phase difference at different times. However, applications of DInSAR are limited by some drawbacks such as spatial and temporal decorrelation, atmosphere disturbance delay, and DEM error, especially at mountain areas [1， 2]. In order to overcome these limitations, several advanced techniques have been proposed, such as Persistent Scatterer Interferometry (PSI)[3，4] and Small baseline Subset Algorithm (SBAS)[5]. However, those above methods have some limitations in landslide monitoring due to low density of PSs or coherent points and their inhomogeneous distribution. To improve the spatial density of the measurement points, Distributed Scatterers Interferometry (DSI) has been proposed to monitor the surface deformation of large scale suburb areas [6，7]. Thanks to the successfully launching of TanDEM-X (TDX), the twin of the TerraSAR-X (TSX), high accuracy DEM without temporal decorrelation and atmospheric distortion can be obtained from the first bistatic space-borne SAR system[8].

In this study, we try to monitor the deformation of the giant landslide at Wenjiagou after Wenchuan earthquake using time-series InSAR technique on DSs. TDX and TSX bistatic SAR data acquired on Feb. 1, 2013 are processed to generate high precision DEM of the post-landslide in this work (no external DEM is used) [9]. DSs can be identified using both classified information and statistical characteristics. A series of Radarsat-2 HH polarization images collected in Wenjiagou from 2014.6 to 2014.9 are used to get the deformation of the giant landslide. Experimental result shows that the landslide moves during the observation.

2. METHOD

The block diagram of the method is shown in Fig.1. High precision DEM can be generated from TDX and TSX data using InSAR technique. Combining classified and statistical information, DSs can be selected from calibrated amplitude images. After constructing triangulation network on DSs which are in landslide area, deformation rate and elevation error are retrieved using conventional PSI.

2.1. DEM from CoSSC Product

High quality DEM can be obtained from the Coregistered Single look Slant range Complex (CoSSC) generated from TDX-TSX bistatic system using conventional InSAR technique. Thanks to the bistatic system, the interferometric phase is free from temporal, motion and atmosphere decorrelation. The InSAR process flow chart for TDX and TSX data contains four main steps as: interferogram generation, interferogram flatten, phase unwrapping, and phase to height conversion and geocoding [10].

Proc. 'Fringe 2015 Workshop', Frascati, Italy
23–27 March 2015 (ESA SP-731, May 2015)

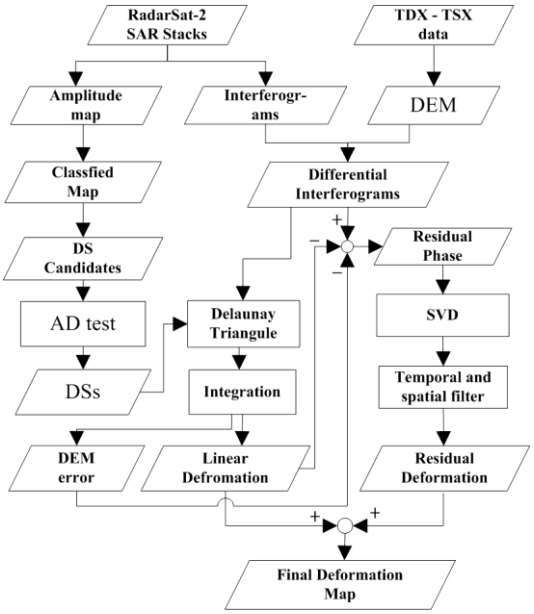

Figure .1 Block diagram of the proposed method.

2.2. DS selection

DSs are statistical homogeneous pixels (SHP) sharing the same behaviour corresponding to non-cultivated land with short vegetation and soil area. Water and forest area in the image are also homogeneous pixels, but not belonging to DSs. A prior classification map of the region can be of great help for DSs selection. In this paper, we obtain the classification map by utilizing mean amplitude map of the SAR images to identify potential DSs areas. The IsoData method is applied to generate classification map in our experiment.

To identify if two pixels are homogenous, we use their amplitude vectors obtained from the stack of SAR amplitude images (in this paper RadarSat-2 SAR stack images) to calculate the empirical cumulative distribution functions and apply a statistical test to compare the distributions. The Anderson-Darling (AD) test has been proven to have better performance than Kolmogorov-Smirnov (KS) test [11]. Thus, AD test is adopted in this paper. For each candidate in the image, its statistical homogeneous pixels are identified, which can be applied to adaptive filtering as well as estimation of complex coherence value. And then, those DS pixels are selected for further processing, which possess an average coherence greater than a certain threshold and have a minimum number of SHP.

2.3. Deformation and topography estimation

After DSs are identified, those selected pixels are should connected to reduce the Atmosphere Phase Screen (APS) effects. Considering the difference between the landslide body and the other stable area, network is constructed on the points in landslide area instead of all the selected points in the image.

Once Delaunay network is constructed on DSs, the parameters of selected points, namely, deformation rate and DEM error can be estimated using conventional PSI [3]. Generally, the phase difference between two neighbouring pixels, x and y, on each edge of network in the kth interferogram can be expressed as the following model:

$$\Delta\varphi^k_{\mathrm{mod}el} = \frac{4\pi}{\lambda}\cdot T^k\cdot\Delta v_{(x,y)} + \frac{4\pi}{\lambda R\sin\theta}\cdot B^k_{\perp}\cdot\Delta\varepsilon_{(x,y)} \quad (1)$$

Where T^k, $B^k_{\perp}$, R and θ denote time baseline, normal baseline, slant range, and incidence angle, respectively; λ is the wavelength and Δv, $\Delta\varepsilon$ are the deformation rate variation and the elevation error variation of two neighbouring pixels.

The differential deformation velocity and height error of the neighbouring pixels can be generated by maximizing the absolute value of ξ ,

$$\xi = \left|\frac{1}{N}\sum_{k=1}^{N}\exp\left[j\cdot(\Delta\phi^k_{phase} - \Delta\phi^k_{\mathrm{mod}el})\right]\right| \quad (2)$$

Where N is the number of interferograms, $\Delta\phi^k_{phase}$ is the phase difference of the neighbouring two points in the k^{th} interferogram. The maximum of the absolute value of (2) is called temporal coherence.

Once the estimation of deformation parameter of all edges has been done, the deformation velocity and DEM error of all the validate points can be obtained through integration step.

3. STUDY AREA AND DATA

Wenjiagou giant landslide, the second largest landslide in the Wenchuan earthquake event, is located in an EW deep-cup gully of Mianyuan River in Qingping town, Mianzu city, Sichuan province as shown in Fig.2. Before the landslide event, Wenjiagou Mountain was covered by rich vegetation and the hill slope was stable. During the earthquake, rock masses slid with a high speed in a short time and moved forward to be thrown, which is shown in Fig.2. Red line displays the boundary of the landslide.

The mass debris deposition of the landslide in the gully can be potential threat to the safety of the local people in rainy season (Fig. 3(A) and (B)). Although some man-made constructions (Fig .3(C) and (D)) are used to control the mass debris, some of the mass debris are eroded by rain water in rainy season, which destructs the landslide construction (Fig. 3(E) and (F)).

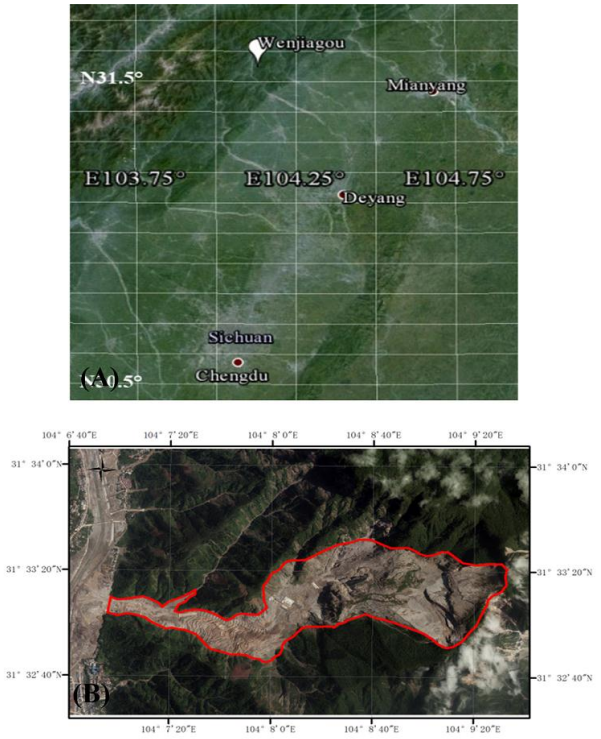

Figure.2 A: Location of the landslide; B: The air-optical image of Wenjiagou.

Figure. 3 Field investigation pictures of the landslide.

In order to get the high precision DEM of the wenjiagou after landslide, CoSSC data from TDX and TSX bistatic system acquired on Feb. 1st, 2013 is processed. The amplitude maps of the master and slave images in Wenjiagou landslide area are shown in Fig. 4. The pixel spacing of range and azimuth is 1.7 m and 2.4m, respectively. Five Radarsat-2 ascending images acquired from Jue 2014 to Sep 2013 with a insidence angle of 36.6 degrees and 'HH' polarization have been processed to obtain the movement information. The pixel spacing of range and azimuth is 2.07 m and 1.33m, respectively. The SAR amplitude image (about 4×5 km^2) averaged from all the images of the study area is shown in Fig.5. 10 interferometric pairs are combined to generate interferograms based on a maximum perpendicular baseline of 200 m and a maximum temporal baseline of 200 days.

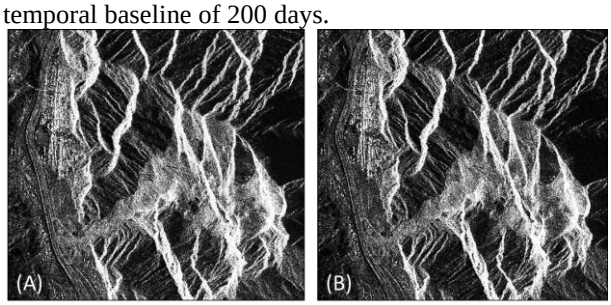

Figure. 4 Amplitude maps of the CoSSC product: (A) the master image; (B) the slave image

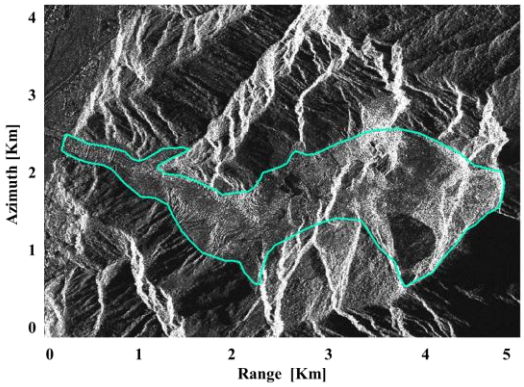

Figure.5 Mean amplitude image of the landslide and landslide boundary.

4. EXPERIMENTAL RESULT

TDX and TSX bistatic data are processed by InSAR technique described in section 2.1. After interferogram phase is flattened, the minimum cost flow method is applied to unwrap the interferogram phase. Once the phase is unwrapped, an elevation map in SAR coordinates is obtained. The final DEM from CoSSC data is shown in Fig. 6. After that, the DEM is converted to the interferometric phase in Radarsat-2 coordinate system.

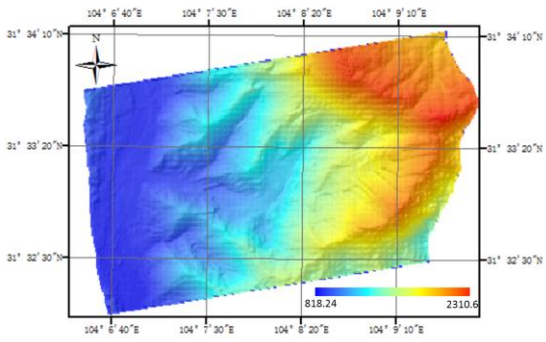

Figure. 6 DEM obtained from CoSSC Data by InSAR technique

In this experiment the unsupervised IsoData method is used to generate classification map based on the mean amplitude image of Radarsat-2. By removing the non-DSs classes, DS candidates are obtained. Subsequently, AD test with a window of 15 ×15 is applied to select the DSs which have an average coherence larger than 0.5 and the number of SHP larger than 120. 362006 DSs have been selected by the proposed selection strategy. And only the DSs which are in the landslide area are processed for deformation estimation as shown in Fig 7. It is shown that DSs are uniformly distributed in the landslide area, which is suited for subsidence monitoring.

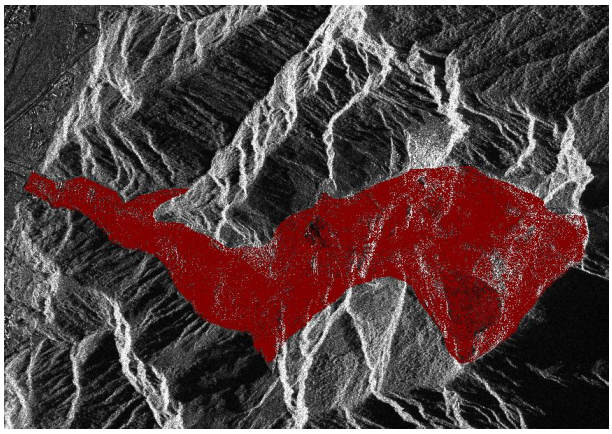

Fig.7 Selected DSs

Fig. 8 shows the post-seismic deformation velocity over the landslide area during the observation. The deformation velocity on DSs over the landslide area indicates a different displacement pattern within the landslide range. In the slope failure area of the landslide the movement rate is very small. In the central of the landslide area obvious movement is detected with maximum velocity reach to 7cm/year. It is because that the main components of the slope failure area of the landslide are exposed rocks, which are stable and difficult to move. In the central of the landslide, the main component is loose mass depositing, which is easy to move after strong rain fall in rainy season. It is suggested that although some man-made construction are used to fix those debris, those areas are also moving in the rain season.

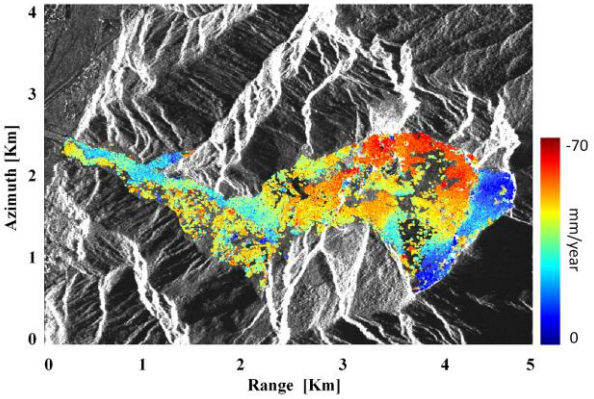

Figure.8 deformation rate at DSs

5. CONCLUSION

This paper has presented an approach to retrieve ground deformation over landslide area using TDX-TSX and Radarsat-2 data. High precision DEM of Wenjiagou is obtained from TDX-TSX data using InSAR method. DSs have been efficiently identified by the selecting strategy using classified information and statistical characteristics. The experimental results show that there are obvious ground movement detected in the depositing area of the landslide during the observation. It is suggested that although some man-made construction are used to fix those debris, those areas are also moving in the rain season. Further work will focus on the parameter step using seasonal phase model, as well as collecting the ground truth data to validate the estimated deformation result.

6. ACKNOWLEDGEMENTS

This work was supported by the National Natural Science Foundation of China under Grants 41271425 and 41331176.

7. REFERENCE

[1] H. A. Zebker, P. A. Rosen, and S. Hensley, "Atmospheric effects in interferometric synthetic aperture radar surface deformation and topographic maps,"*J. Geophys. Res*, vol. 102, pp. 7547-7563, 1997.

[2] H. A. Zebker, J. Villasenor, "Decorrelation in interferometric radar echoes." *IEEE Trans. Geosci. Remote Sens.*, vol. 30, no. 5, pp. 950-959, 1992.

[3] A. Ferretti, C. Prati, and F. Rocca, "Permanent scatterers in SAR interferometry," *IEEE Trans. Geosci. Remote Sens.*, vol. 39, no. 1, pp. 8-20, 2001.

[4] A. Hooper, H. Zebker, P. Segall, and B.Kampes, "A new method for measuring deformation on volcanoes and other natural terrains using InSAR persistent scatterers," *Geophys. Res.Lett.*, vol. 31, no. 23, 2004.

[5] P. Berardino, G. Fornaro, R. Lanari, and E.Sansosti, "A new algorithm for surface deformation monitoring based on small baseline differential SAR interferograms," *IEEE Trans.*

Geosci. Remote Sens., vol. 40, no. 11, pp. 2375-2383, 2002.
[6] A. Ferretti, A. Fumagalli, F. Novali, C. Prati, F. Rocca, and A. Rucci, "A new algorithm for pro-cessing interferometric data-stacks: Squeesar," *IEEE Trans. Geosci. Remote Sens.*, vol. 49, no. 9, pp. 3460-3470, 2011.
[7] K. Goel and N. Adam, "A Distributed Scatterer Interferometry Approach for Precision Monitoring of Known Surface Deformation Phenomena," *IEEE Trans. Geosci. Remote Sens.*, vol.52, no. 9, pp. 5454-5468, 2014.
[8] G. Krieger, A. Moreira, H. Fiedler, I. Hajnsek, M. Werner, M. Younis, et al., "TanDEM-X: A satellite formation for high-resolution SAR interferometry," *IEEE Trans. Geosci. Remote Sens.*, vol. 45, pp. 3317-3341, 2007.
[9] Y. Tang, Z. Zhang, C. Wang, H. Zhang, F. Wu, and M. Liu, "Characterization of the giant landslide at wenjiagou by the InSAR technique using TSX-TDX CoSSC Data", *Landlides*.(in review)
[10] C. Rossi, F. Rodriguez Gonzalez, T. Fritz, N. Yague-Martinez, and M. Eineder, "TanDEM-X calibrated Raw DEM generation," *ISPRS J. Photogram. Remote Sens.*, vol.73, pp.20-20, 2012.
[11] A. Parizzi, and R. Brcic, "Adaptive InSAR stack multilooking exploiting amplitude statistics: a comparison between different techniques and practical results," *IEEE Trans. Geosci. Remote Sens.*, vol. 8, no. 3, pp.441-445, 2011.